Luminescence spectra of laser-induced cavitation bubbles near rigid boundaries

Emil A. Brujan* and Gary A. Williams
Department of Physics and Astronomy, University of California, Los Angeles, California 90095, USA
(Received 21 December 2004; published 12 July 2005)

The luminescence spectra of laser-induced cavitation bubbles near rigid boundaries are measured for various relative distances between the bubble and the boundaries. We find that the luminescence spectra of bubbles collapsing near a single boundary consist only of a blackbody continuum. Luminescence from bubbles collapsing between two parallel rigid boundaries contains OH^- emission bands similar to those found in multibubble sonoluminescence. In both cases, the bubble interior temperature deduced from blackbody fits decreases with the distance between bubble and boundary. The shape instabilities of the collapse near a boundary and the consequent presence of high-velocity jets inside the bubble at its minimum volume are discussed in connection with the generation of the OH^- radicals.

DOI: 10.1103/PhysRevE.72.016304 PACS number(s): 78.60.Mq, 47.55.Bx, 47.55.Dz, 47.20.Ma

I. INTRODUCTION

The emission of light from collapsing bubbles in water is an interesting phenomenon that is still not well understood. In the presence of a high-amplitude sound field this is known as single- or multibubble sonoluminescence (SBSL or MBSL) [1]. A similar type of luminescence can be observed without a sound field present, in the collapse of bubbles that are formed by a focused laser pulse [2–4]. Single-bubble sonoluminescence has been shown to have a continuum emission spectrum with no discernible atomic or molecular lines [5]. An estimate the interior bubble temperature at the moment of light emission can be obtained by fitting the spectra to a blackbody form [4,6] , and in general this yields results of ~8000 to 50 000 K, depending on the gas in the bubble. In contrast, the light emitted from cavitating multibubble sonoluminescence often contains well-defined lines and bands superimposed upon the continuum. In particular, the MBSL spectra of water contain prominent emission lines of the excited hydroxyl (OH^-) bands at 310 nm [7]. Based on the measurements of the relative intensities of emission lines from different bands in metal complexes, bubble interior temperatures of ~5000 K have been obtained for MBSL [8].

The luminescence from the laser-induced bubbles is unique in the sense that, depending on the maximum bubble size, it displays both the characteristics of SBSL and MBSL. For relatively small bubbles ($R_{max} < 0.6$ mm) the luminescence spectrum is a smooth continuum similar to SBSL, with a blackbody temperature of about 8000 K. For large bubbles ($R_{max} > 1$ mm) the OH^- band at 310 nm is also observed, as in MBSL. Since shape instabilities such as jets and fission into two bubbles were also observed close to the collapse point of these bubbles [3,4], it was speculated in Ref. [4] that the OH^- emission might be correlated with the onset of the shape instabilities. A similar speculation was made in Ref. [7] for MBSL, since large unstable bubbles are known to be present in the chaotic multibubble cavitation. A connection between shape instabilities and the bubble luminescence was observed by Ohl *et al.* [2]. They studied the generation of laser-induced bubbles at various distances from a flat rigid boundary, which is well known to induce a jet instability in the bubble collapse when it is close to the wall [9]. They observed that the strength of the luminescence dropped rapidly to insignificant levels when the distance between bubble and boundary was reduced to less than 3–4 times the maximum bubble radius.

In this paper, we present measurements of the interior temperature of laser-induced bubbles collapsing near rigid walls, using blackbody fits to the luminescence spectra. Two geometries were investigated in the present study. In the first the bubble was generated at different distances from a flat rigid wall. The second geometry consists of two parallel flat rigid walls, with the bubble being initiated between the walls at equal distance from them. The significant parameter of this study is the nondimensional stand-off distance γ, defined as the ratio of the initial location of the bubble from the boundary divided by the maximum bubble radius.

II. EXPERIMENT

Individual bubbles were generated in a stainless-steel cuvette formed by boring three 40 mm diameter intersecting holes through a cubical block of sides 68 mm, where the four side holes are fitted with millimeter-thick quartz windows attached with epoxy to mounting flanges sealed with rubber O rings. The bottom hole of the cell has a lens mounted in the same manner that is 30 mm in diameter and has a focal length of 35 mm. The lens focuses a 6 ns pulse from a Q-switched Nd:YAG laser at 1064 nm into the center of the cell. The cell is filled with 18 MΩ, 0.2-μm-filtered water at room temperature, 22 °C. The focused laser pulse ionizes the water (probably initiated by an impurity), creating a breakdown plasma that is 50–100 μm in diameter and lasts 50–100 ns [10]. The energy deposited then appears as an expanding bubble, with the gas in the bubble consisting primarily of the ionization products atomic hydrogen and oxygen. After reaching its maximum size the bubble col-

*Permanent address: University Polytechnica of Bucharest, Department of Hydraulics, Spl. Independentei 313, sector 6, 060042 Bucharest, Romania.

lapses, heating the gas inside, and the luminescence pulse is emitted at the minimum-radius collapse point [3,4]. The bubble size is determined by an indirect measurement using the collapse time T_c of the bubble at very large values of γ. The maximum radius $R_{\max}$ of a spherical bubble situated in a liquid of infinite extent is given by [11]

$$R_{\max} = 0.55\sqrt{\frac{p - p_v}{\rho}}T_c, \quad (1)$$

where ρ is the density of the liquid, p the static pressure, and p_v the vapor pressure of the liquid. Equation (1) assumes that the expansion and collapse phases of the bubble oscillation are symmetric. This condition is fulfilled in the present study, because the bubbles are produced by laser pulses considerably shorter than the bubble collapse time. The collapse time of the bubble was obtained by measuring the time interval between the luminescence pulse emitted during optical breakdown and the bubble luminescence, using a photomultiplier tube (Hamamatsu H6780). Boundary walls made of 1-mm-thick Plexiglass are inserted from the top of the cell using adjustable positioners. The maximum bubble radius and the distance s between the laser focus and the boundary yield the non-dimensional stand-off parameter $\gamma = s/R_{\max}$. It should be noted here that close to boundaries, where the expanded bubble is nonspherical, $R_{\max}$ represents the radius of a spherical bubble with the same volume (equivalent spherical radius). We thus assume that the maximum bubble volume does not change with variation of γ at constant laser pulse energy. The equivalent spherical radius is, hence, assumed to be independent of γ. On the other hand, a boundary in the vicinity of a bubble leads to a prolongation of the bubble collapse time. We note, however, that for $\gamma > 3$, the error in estimating the maximum bubble radius is smaller than 5% [12], so that, in this range, the maximum bubble radius can be estimated with a reasonable accuracy. In this experiment, the maximum bubble radius was held constant at a value $R_{\max} = 0.75 \pm 0.05$ mm, with a collapse time T_c of about 140 μs. To obtain a spectrum, light emitted from the bubble along the direction parallel to the two boundaries was collected and collimated by a MgF_2-coated paraboloid mirror. A second paraboloid mirror focuses the collimated beam into the entrance slits of a 0.3 m spectrometer (SpectraPro 300I, Acton Research Corporation) with a gateable intensified charge-coupled device (ICCD) detector. To reject light at higher orders, long-pass filters at either 300 or 500 nm were placed in front of the spectrometer. To get a sufficient signal for a spectrum, the light emitted was averaged over 25 bubbles. The raw spectra are corrected for the detector sensitivity and for absorption losses in the cell windows and spectrometer, using a calibration curve derived from D_2 and quartz lamps. The pressure amplitude of the acoustic transients emitted during bubble collapse was measured by using a PVDF hydrophone (Precision Acoustics) with a rise time of 25 ns, an active area of 0.8 mm^2, and a sensitivity of 12 mV/kPa. The hydrophone was connected to a digital oscilloscope (Hewlett-Packard Infinium) with 1 MΩ input impedance to ensure proportionality between voltage and pressure. Far field measurements were performed with the hydrophone placed at a distance of 10 mm from the emission center. In the far field, the portion of the shock wave intersecting the active area of the pressure transducer can be approximated by a plane wave, and the hydrophone measurements are thus more accurate.

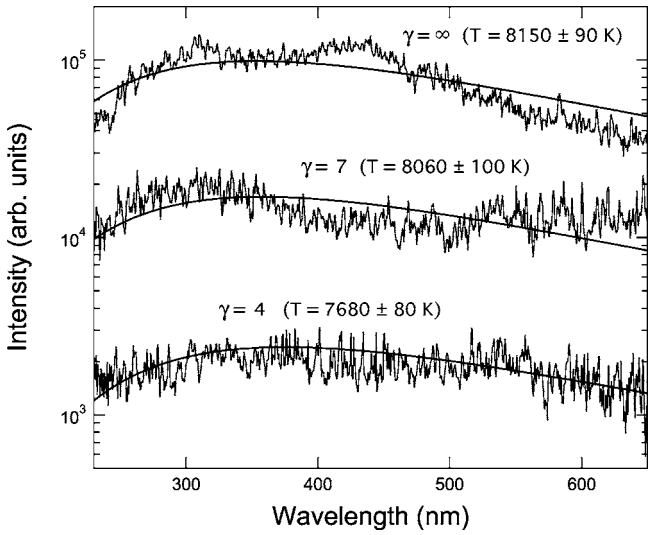

FIG. 1. Luminescence spectra of bubbles collapsing near a single rigid wall for various relative distances between bubble and boundary. The spectra are offset in the vertical direction for better visualization.

III. RESULTS

Figure 1 shows the luminescence spectra of laser-induced bubbles near a rigid boundary for $\gamma = \infty$ (spherical bubble), $\gamma = 7$ and $\gamma = 4$, respectively. The spectral radiance decreases toward the infrared, and the major part of the energy is captured in the wavelength range $\lambda < \lambda_{IR} \approx 700$ nm. On the other hand, the water surrounding the bubble strongly absorbs UV light below $\lambda_{UV} \approx 200$ nm so that this portion of the emitted light is lost. Each spectrum consists of a continuum, and the spectral-intensity distributions can be fitted to that of a blackbody radiator with temperatures ranging from 8150 K for spherical bubbles [4] to about 7700 K for $\gamma = 4$. For $3 < \gamma < 4$, the intensity of the light emitted by the bubble was too small to obtain a spectrum. For $\gamma < 3$, no light emission was observed, in agreement with the previous results [2].

A significant difference is observed when the bubble is initiated between two rigid boundaries (Fig. 2). The spectrum of the bubble luminescence consists now of both a continuum and a peak at 310 nm which appears as the bubble approaches the walls. The 310 nm peak is not visible in the $\gamma = 7$ data but is quite prominent at $\gamma = 4$. In the latter case, the spectral-intensity distribution can still be roughly approximated by a blackbody spectrum with a temperature of about 7400 K, although the presence of spectral lines shows that a black-body assumption is probably not completely accurate. The 310 nm peak appears to be the same emission band from the OH^- radical that was observed previously [4] in laser bubbles with maximum size greater than 1 mm, and in MBSL [7].

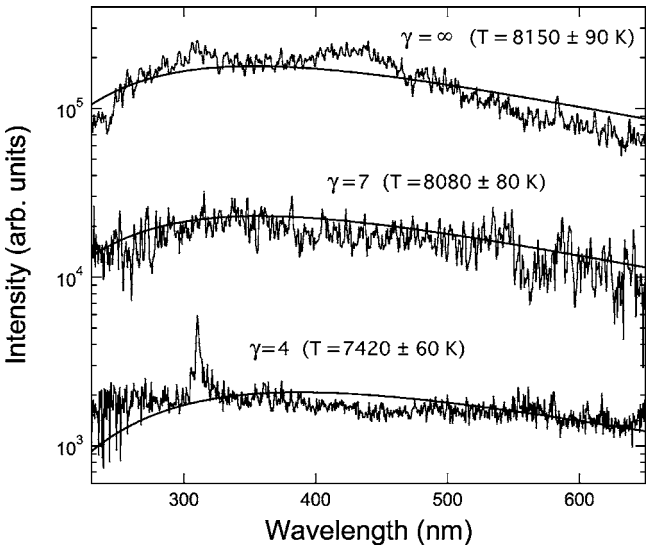

FIG. 2. Luminescence spectra of bubbles collapsing between two parallel rigid boundaries. The bubbles are initiated at equal distance from boundaries. Intensities have been scaled arbitrarily between the different curves.

Figure 3 shows the maximum pressure amplitude p_{max} of the acoustic transients emitted during collapse of a bubble near a rigid wall and between two parallel walls, respectively, as a function of γ. In both cases p_{max} decreases with the stand-off parameter γ. Although there is a large scatter of the results it can be seen that the largest reduction occurs when the bubble is initiated between two parallel walls for γ values smaller than about 5. At very large γ values ($\gamma > 8$) the maximum amplitude of the acoustic transients emitted during first bubble collapse exhibits an almost constant plateau at about 1.2 MPa, indicating that the bubble behavior is similar to that in a fluid of infinite extent.

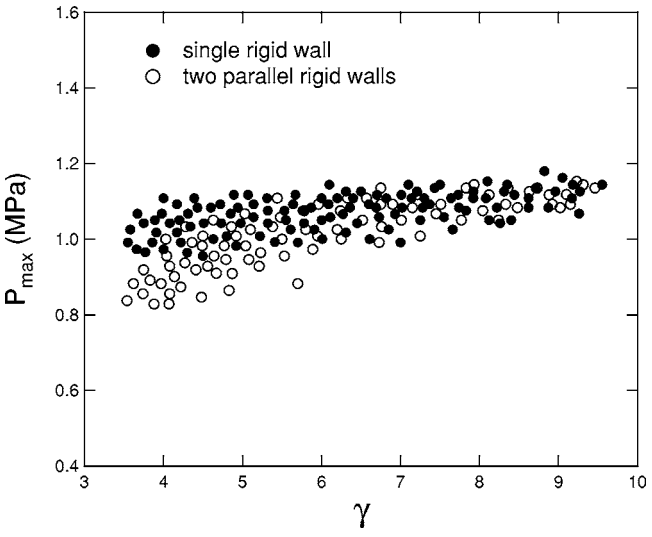

FIG. 3. Maximum amplitude of the acoustic transients emitted during bubble collapse near a rigid boundary and between two parallel rigid boundaries. The hydrophone is placed parallel to the boundaries, 10 mm away from the laser focus.

IV. DISCUSSION

The dependence of the bubble interior temperature on the boundary conditions can be understood in a heuristic manner. A spherical bubble produced in an unconfined liquid retains its spherical shape while oscillating, and the bubble collapse takes place at the site of bubble formation. The collapse compresses the bubble content into a very small volume, thus generating a very high pressure that can exceed 1 GPa for an approximately spherical bubble [12]. The rebound of the compressed bubble interior leads to the emission of a strong pressure transient into the surrounding liquid that can evolve into a shock wave. However, when the bubbles are formed near a material boundary, the collapse is asymmetric and associated with the formation of one or two high-speed liquid jets that concentrate the bubble energy at some distance from the locus of bubble formation. When the bubble collapses near a single rigid boundary, the jet is directed towards the boundary [13,14]. The bubble collapse between two parallel rigid boundaries is characterized by the formation of an annular flow leading to bubble splitting and the generation of two high-speed axial liquid jets directed toward the boundaries [15,16]. The temperature inside a collapsing spherical bubble is obviously the highest, because during collapse the flow of the surrounding liquid is directed into a small region, giving rise to strong energy focusing and high volume compression. The motion of a bubble produced near a rigid boundary is less spherical leading to a lower compression and weaker shock wave emission during rebound. A bubble that is produced between two parallel rigid boundaries has even a smaller compression, because more energy is used up in the annular flow and axial liquid jets developed after bubble splitting. The slowing of the collapse in this manner is likely to reduce even more the ambient temperature in the gases in the bubble.

The most interesting feature of the luminescence spectra of bubbles collapsing between two parallel rigid boundaries is the occurrence of the OH^- radical. There have been several attempts to construct a model for the OH^- formation and a variety of suggestions have emerged, principally due to a paucity of experimental details. Most models invoke adiabatic compression of the gas inside the bubble, which leads to high interior temperatures. A first model assumes that while a highly thermally stable end-product H_2 is formed by recombination of H^+ ions, a relatively labile end-product of recombination of OH^- radicals, H_2O_2, may undergo O-O bond homolysis in the interfacial region of the bubble to regenerate OH^- radicals (see, for example, Ref. [17]). However, considering that molecular recombination is a very slow process on the microsecond time scales of our bubbles, and that the OH^- band was not observed in the spectrum of spherical bubbles, this scenario is unlikely. In a competing model, Mark *et al.* [18] considered that if the bubble interior temperature is high and the number of water molecules inside bubbles exceeds the number of radicals, a considerable number of H^+ ions will be converted to OH^- radicals by $H^+ + H_2O \rightarrow H_2 + OH^-$. A prerequisite of this model is the complete penetration of a high-speed liquid jet into the bubble at its minimum volume where the temperature has the highest value. At first sight this scenario can be ruled out,

since the OH^- radical was not generated when the bubble collapsed near a single rigid wall. In this case, a possible explanation for the smooth continuum spectrum is the absence of a well-defined jet inside the bubble prior to the collapse point. Although no direct observation is available in the literature, the numerical calculations of Pearson *et al.* [19] indicate for $\gamma > 4$ a deceleration of the liquid within the jet due to compression of gas within the bubble as its volume decreases, then subsequent acceleration of the remaining surface of the bubble (which does not bound the liquid jet) due to high internal pressures.

On the other hand, ultra-high-velocity jets can be initiated during bubble collapse between two rigid boundaries, and two factors may contribute to this process. First, the driving pressure is larger than in the case of a single boundary. The jet flow near a boundary is driven by the pressure from a stagnation point above the bubble [20]. A bubble collapsing between two parallel walls achieves an oblate shape in an initial collapse stage. This leads to the formation of an annular flow which is further accelerated in the final collapse stage by a high pressure ring (see, for example, Ref. [21]). Ultra high-velocity jets emanating during the collapse of an oblate bubble have been theoretically predicted by Voinov and Voinov [22]. A jet velocity of 640 m/s was predicted for an initial elongation of 17%. Second, the redirection into an axial jet is also mediated by the shock waves emitted upon collapse by the cavities formed after the bubble splitting. A clear visualization of this process can be found for bubbles oscillating near an elastic boundary where jet velocities as high as 960 m/s were generated [23]. Obviously, such high velocity jets are capable of penetrating the interior of the cavities formed after bubble splitting even before they reach the minimum volume. It is interesting to note here that Baghdassarian *et al.* [4] speculate on a connection between bubble splitting and the OH^- emission in the spectrum for large bubbles (of radius 1–2 mm) created in a liquid of infinite extent. The bubble splitting there is probably a consequence of an oblate shape of the bubble during the collapse phase which in turn is caused by an elongated plasma during the initial optical breakdown.

The fact that at $\gamma = 7$ the OH^- band was not observed in Fig. 2 for bubbles collapsing between two parallel rigid walls is not surprising. Recent numerical and experimental investigations of Ishida *et al.* [16] have indicated that for $\gamma > 5$ the influence of the boundaries on the bubble motion is negligibly small. This result is also confirmed by the present acoustic measurements. Therefore, the characteristics of the spectrum are similar to those of spherical bubbles, i.e., without an emission band from the OH^- molecular complex.

In a cloud of bubbles, as encountered in MBSL studies, a greater probability for the occurrence of ultra-high-velocity jets is possible. Bubble splitting leading to the formation of high-speed liquid jets due to the presence of other bubbles have been demonstrated by Blake *et al.* [24]. This process would presumably lead to the same OH^- emission as described above. Another accelerating effect on the jet velocity may be the interaction of an acoustic transient emitted by bubbles collapsing in the neighborhood of the jetting bubble [13]. It is well known that a strong acoustic transient hitting a bubble will induce collapse of the bubble, forming a high-speed liquid jet that completely penetrates the bubble at its minimum volume. This process is independent of any boundary in the vicinity of the bubble and the direction of the jet is the same as the propagation direction of the acoustic wave.

V. CONCLUSIONS

We have found that the spectrum of a bubble collapsing near a single rigid boundary shows only a smooth continuum. In contrast, the luminescence spectrum of a bubble collapsing between two parallel rigid boundaries shows an emission band from the OH^- radical at 310 nm, similar to that observed in the MBSL spectra of water. The appearance of the OH^- band in the spectrum may be related to ultra high-velocity jets that accompany the splitting of the bubble into two just prior to the minimum-radius collapse point. For the single boundary the jet is apparently only formed after the collapse point, when the gases have cooled and OH^- can no longer be formed. In both cases, the spectral radiance can be fitted with a blackbody curve at a temperature that decreases with the relative distance between bubble and boundary.

ACKNOWLEDGMENTS

This work was supported by the National Science Foundation, Grant No. DMR 01-31111. E. A. Brujan acknowledges support from the Fulbright Scholars Program of the Council for International Exchange of Scholars.

[1] M. Brenner, S. Hilgenfeldt, and D. Lohse, Rev. Mod. Phys. **74**, 425 (2002); W. Moss, D. Clarke, and D. Young, Science **276**, 1398 (1997); Y. T. Didenko and S. P. Pugach, J. Phys. Chem. **98**, 9742 (1994).

[2] C. D. Ohl, O. Lindau, and W. Lauterborn, Phys. Rev. Lett. **80**, 393 (1998).

[3] O. Baghdassarian, B. Tabbert, and G. A. Williams, Phys. Rev. Lett. **83**, 2437 (1999).

[4] O. Baghdassarian, H.-C. Chu, B. Tabbert, and G. A. Williams, Phys. Rev. Lett. **86**, 4934 (2001).

[5] R. Hiller, S. J. Putterman, and B. P. Barber, Phys. Rev. Lett. **69**, 1182 (1992).

[6] G. Vazquez, C. Camara, S. Putterman, and K. Weninger, Phys. Rev. Lett. **88**, 197402 (2002).

[7] T. Matula, R. Roy, P. Mourad, W. McNamara, and K. Suslick, Phys. Rev. Lett. **75**, 2602 (1995).

[8] W. B. McNamara, Y. T. Didenko, and K. S. Suslick, Nature (London) **401**, 772 (1999).

[9] V. Kamath and A. Prosperetti, J. Acoust. Soc. Am. **94**, 248 (1993); L. A. Crum, *ibid.* **95**, 59 (1994).

[10] O. Baghdassarian, Ph.D. thesis, UCLA, 2001.
[11] Lord Rayleigh, Philos. Mag. **34**, 94 (1917).
[12] A. Vogel, W. Lauterborn, and R. Timm, J. Fluid Mech. **306**, 299 (1989).
[13] Y. Tomita and A. Shima, J. Fluid Mech. **169**, 535 (1986).
[14] E. A. Brujan, G. S. Keen, A. Vogel, and J. R. Blake, Phys. Fluids **14**, 85 (2002).
[15] G. L. Chahine, Appl. Sci. Res. **38**, 187 (1982).
[16] H. Ishida, C. Nuntadusit, H. Kimoto, T. Nagagawa, and T. Yamamoto, in *CAV 2001: Proceedings of 4th Int.Symp. Cavitation*. California Institute of Technology, Pasadena, CA. http://cav2001.library.caltech.edu/426/
[17] R. E. Verral and C. M. Sehgal, in *Ultrasound: Its Chemical, Physical and Biological Effects*, edited by K. S. Suslick (VCH, New York), pp. 227-286.
[18] G. Mark, A. Tauber, R. Laupert, H.-P. Schuchmann, D. Schultz, A. Mues, and C. von Sonntag, Ultrason. Sonochem. **5**, 41 (1998).
[19] A. Pearson, J. R. Blake, and S. R. Otto, J. Eng. Math. **48**, 391 (2004).
[20] J. R. Blake, B. B. Taib, and G. Doherty, J. Fluid Mech. **170**, 479 (1986).
[21] E. A. Brujan, A. Pearson, and J. R. Blake, Int. J. Multiphase Flow, **31**, 302 (2005).
[22] O. V. Voinov and V. V. Voinov, Sov. Phys. Dokl. **21**, 133 (1976).
[23] E. A. Brujan, K. Nahen, P. Schmidt, and A. Vogel, J. Fluid Mech. **433**, 251 (2001).
[24] J. R. Blake, P. B. Robinson, A. Shima, and Y. Tomita, J. Fluid Mech. **255**, 707 (1993).